HHS Public Access

Author manuscript

J Gastroenterol Hepatol. Author manuscript; available in PMC 2015 August 27.

Published in final edited form as:

J Gastroenterol Hepatol. 2013 October ; 28(10): 1660–1668. doi:10.1111/jgh.12291.

Ceramide inhibitor myriocin restores insulin/insulin growth factor signaling for liver remodeling in experimental alcohol-related steatohepatitis

Diana Lizarazo[*], **Valerie Zabala**[*], **Ming Tong**[*], **Lisa Longato**[*], and **Suzanne M. de la Monte**[†]

[*]Liver Research Center, Division of Gastroenterology and Department of Medicine, Rhode Island Hospital and the Warren Alpert Medical School of Brown University, Providence, RI, USA

[†]Liver Research Center, Divisions of Gastroenterology and Neuropathology and Departments of Medicine, Pathology, Neurology, and Neurosurgery, Rhode Island Hospital and the Warren Alpert Medical School of Brown University, Providence, RI, USA

Abstract

Background and Aim—Alcohol-related liver disease (ALD) is mediated in part by insulin resistance. Attendant dysregulation of lipid metabolism increases accumulation of hepatic ceramides that worsen insulin resistance and compromise the structural and functional integrity of the liver. Insulin and insulin growth factor (IGF) stimulate aspartyl-asparaginyl-β-hydroxylase (AAH), which promotes cell motility needed for structural maintenance and remodeling of the liver. AAH mediates its effects by activating Notch, and in ALD, insulin/IGF signaling, AAH, and Notch are inhibited.

Method—To test the hypothesis that in ALD, hepatic ceramide load contributes to impairments in insulin, AAH, and Notch signaling, control and chronic ethanol-fed adult Long–Evans rats were treated with myriocin, an inhibitor of serine palmitoyl transferase. Livers were used to assess steatohepatitis, insulin/IGF pathway activation, and expression of AAH–Notch signaling molecules.

Results—Chronic ethanol-fed rats had steatohepatitis with increased ceramide levels; impairments in signaling through the insulin receptor, insulin receptor substrate, and Akt; and decreased expression of AAH, Notch, Jagged, Hairy–Enhancer of Split-1, hypoxiainducible factor 1α, and proliferating cell nuclear antigen. Myriocin abrogated many of these adverse effects of ethanol, particularly hepatic ceramide accumulation, steatohepatitis, and impairments of insulin signaling through Akt, AAH, and Notch.

Conclusions—In ALD, the histopathology and impairments in insulin/IGF responsiveness can be substantially resolved by ceramide inhibitor treatments, even in the context of continued chronic ethanol exposure.

Correspondence Dr Suzanne M. de la Monte, Pierre Galletti Research Building, Rhode Island Hospital, 55 Claverick Street, Room 419, Providence, RI 02903, USA. Suzanne_DeLaMonte_MD@Brown.edu.

The authors have no conflicts of interest.

Keywords

alcoholic liver disease; aspartyl-asparaginyl-β-hydroxylase-myriocin; ceramides; insulin resistance; Notch; steatohepatitis

Introduction

Alcohol abuse is a leading cause of liver-related morbidity and mortality.[1] Excessive alcohol consumption causes steatohepatitis, which progresses to chronic alcohol-related liver disease (ALD)[2] owing to the combined effects of insulin and insulin-like growth factor (IGF) resistance,[3–5] inflammation, oxidative and endoplasmic reticulum (ER) stress, lipotoxicity with ceramide accumulation, and mitochondrial dysfunction.[3–7] Ethanol-impaired insulin/IGF type 1 (IGF-1) signaling[3,4,8–10] inhibits downstream activation of mitogen-activated protein kinase (MAPK), which supports liver growth and repair, and that of phosphatidyl-inositol-3-kinase (PI3K) and Akt,[3] which promote hepatocellular survival, motility, and metabolism.[11] Ethanol increases activation of glycogen synthase kinase 3β (GSK-3β)[8] and that of phosphatases that negatively regulate receptor tyrosine kinases and PI3K.[8] Therefore, disruption of insulin/IGF signaling accounts for many long-term toxic and degenerative effects of ethanol on the liver.[3,9,12,13]

Aspartyl-asparaginyl-β-hydroxylase (AAH) is an important downstream target of insulin signaling because of its role in regulating cell motility, which is needed for liver remodeling, repair, and regeneration.[4,14–16] AAH is an ~86-kD type 2 transmembrane protein that undergoes physiological cleavage, releasing a ~52–54-kD *C*-terminal fragment that has catalytic (hydroxylase) activity and a smaller ~32–34-kD *N*-terminal fragment that is highly homologous to another protein called Humbug.[17–19] AAH's *C*-terminal catalytic fragment confers cell motility, invasiveness, and adhesion,[14,16] whereas the *N*-terminus of AAH mediates calcium flux between the ER and cytosol via ryanodine receptors[20] and thereby modulates cell adhesion.[14]

The consensus sequence for AAH hydroxylation resides in epidermal growth factor-like domains that are present in proteins such as Notch and Jagged.[21,22] AAH hydroxylation of Notch leads to its proteolytic cleavage and release of the intracellular domain, which translocates to the nucleus, where it binds to transcriptional regulators, displacing corepressors and recruiting coactivators.[23,24] The net effect is to increase expression of target genes such as Hairy–Enhancer of Split (HES) and HES-related proteins.[25] AAH's roles in cell motility and invasion have been linked to activation of Notch networks.[14,26,27] Insulin and IGFs regulate AAH by increasing its mRNA levels, catalytic activity,[14,26,28,29] and protein expression.[15,26,28] Insulin/IGF stimulation causes AAH protein to accumulate in cells owing to inhibition of GSK-3β phosphorylation, which renders AAH susceptible to proteolytic degradation.[27] Ethanol inhibits AAH expression and function by impairing insulin/IGF signaling and increasing GSK-3β activity.[3,29–31]

Consequences of insulin resistance, including dysregulated lipid metabolism,[12,32–34] inflammation,[32] oxidative and ER stress,[6,34] metabolic and mitochondrial dysfunction,[35] decreased DNA synthesis,[4] and increased cell death,[12] contribute to hepatocellular injury

and degeneration and cause ALD to progress.[13] Dysregulation of lipid metabolism is of particular interest because the attendant lipolysis with ceramide accumulation establishes a lipitoxic state. Consequences include further compromise of insulin signaling networks,[36] activation of pro-inflammatory cytokines, inhibition of PI3K-Akt,[37–39] and increase in ER and oxidative stress.[7,33,40]

Ceramides are likely to have an important role in the pathogenesis and progression of ALD, based on reports demonstrating that (i) mice deficient in acidic sphingomyelinase are resistant to ethanol-induced hepatic steatosis;[41] (ii) ceramides inhibit adenosine monophosphate-activated protein kinase (AMPK)[42] and promote local hepatocellular injury,[43] possibly because AMPK reduces ER stress and apoptosis;[44] and (iii) in humans with advanced ALD, hepatic ceramide levels are increased.[5,13] The present study tests the hypothesis that ALD can be treated effectively by inhibiting hepatic ceramide accumulation to disinhibit signaling through insulin/IGF and interrelated pathways. Using an established experimental model of chronic ALD, we assessed the therapeutic effects of myriocin, a potent serine palmitoyl transferase (de novo pathway) inhibitor,[45] on steatohepatitis, insulin signaling, ER stress markers, and activation of AAH–Notch signaling networks in liver.

Methods

The sources of commercial reagents and standard methods are provided in the Supplementary Methods section. The A85E6 and A85G6 mouse monoclonal antibodies to AAH were generated as previously described.[29,30]

Adult male Long–Evans rats were pair-fed with isocaloric liquid diets containing 0% or 37% (caloric content; 9.2% v/v) ethanol for 8 weeks.[4] From weeks 4 through 8 of liquid diet feeding, rats in each group were treated with myriocin (0.3 mg/kg) or saline 3 times per week. Rats were then overnight-fasted and sacrificed to obtain livers for morphologic, biochemical, and molecular studies. Gene expression was measured by quantitative reverse transcription polymerase chain reaction (qRT-PCR) analysis.[46] Protein expression was measured by duplex[5] or multiplex ELISAs. Ceramide immunoreactivity was quantified by ELISA.[5,47] Data (n = 6/group) were analyzed using GraphPad Prism 5 software (Graphpad Prism Software, Inc., La Jolla, CA, USA), and intergroup comparisons were made using repeated-measures one-way analysis of variance (ANOVA) with Tukey's multiple-comparisons post hoc test.

Results

Myriocin ameliorates ALD

Control livers had the expected cordlike architecture and were free of inflammation, steatosis, fibrosis, and cholestasis (Fig. 1a). Myriocin treatment produced subtle changes in control livers, such that hepatocytes were rendered more polygonal, with discrete borders, relative to control + vehicle livers (Fig. 1b). Chronic ethanol-fed rats had steatohepatitis characterized by diffuse hepatocellular cytoplasmic microvesicular lipid vacuoles, dilated sinusoids, multiple foci of lymphomononuclear cell inflammation, and scattered hepatocytes undergoing apoptosis or necrosis (Fig. 1c). Myriocin reduced sinusoidal dilation,

inflammation, and hepatic steatosis. However, foci of apoptosis, low-level inflammation, and evidence of increased cell turnover persisted (Fig. 1d).

Oil Red O (ORO) staining revealed zonal and relatively low levels of hepatocellular lipid accumulation in control livers, irrespective of myriocin treatment (Fig. 2a,b). Chronic ethanol feeding caused striking panlobular hepatic steatosis, with both coarse and fine cytoplasmic lipid droplets (Fig. 2c). Myriocin conspicuously reduced hepatic steatosis, as was evident on ORO staining (Fig. 2d). Results of semiquantitative ORO grading (Supplementary Methods) revealed significantly higher levels of hepatic steatosis in the ethanol + vehicle group relative to all others ($P < 0.0001$) and similarly low levels of hepatocellular ORO staining in the control + vehicle, control + myriocin, and ethanol + myriocin groups (Supporting Information Table S1). Correspondingly, higher levels of hepatic ceramide were measured in ethanol + vehicle relative to control + vehicle livers ($P < 0.001$), whereas myriocin normalized hepatic ceramide levels in the ethanol-fed rats despite continuous ethanol exposure. In contrast, myriocin treatment had no significant effect on hepatic triglyceride content (Supporting Information Table S1).

Myriocin restores hepatic insulin and IGF signaling and downstream activation of Akt pathways in ALD

Multiplex ELISAs were used to measure total (Fig. 3) and phosphorylated (Fig. 4) insulin receptor, IGF-1 receptor (IGF-1R), IRS-1, Akt, GSK-3β, proline-rich Akt substrate 40 kDa (PRAS40), and p70S6 kinase (p70S6K), and single-plex assays were used to measure extracellular signal-regulated kinases 1 and 2 (ERK1/2) and $p^{T202/Y204}$–ERK1/2. The calculated ratios of phosphorylated to total protein (Fig. S1) were used to assess relative levels of phosphorylation.

ANOVA tests demonstrated significant intergroup differences with respect to insulin receptor ($F = 3.1$; $P < 0.05$), IRS-1 ($F = 33.46$; $P < 0.0001$), Akt ($F = 27.74$; $P < 0.0001$), PRAS40 ($F = 4.04$; $P = 0.01$), p70S6K ($F = 20.06$; $P < 0.0001$), and ERK ($F = 15.37$; $P < 0.0001$). In contrast, no significant intergroup differences were observed with respect to IGF-1 receptor (Fig. 3b) or GSK-3β (Fig. 3f). Post hoc Tukey–Kramer tests demonstrated that chronic ethanol feeding reduced hepatic expression of the insulin receptor ($P < 0.05$), IRS-1 ($P < 0.001$), Akt ($P < 0.05$), and p70S6K ($P < 0.001$) (Fig. 3). Although PRAS40 expression was also lower in ethanol-exposed livers, the difference from control did not reach statistical significance. Myriocin abolished the intergroup differences with respect to hepatic expression of insulin receptor and PRAS40, significantly increased expression of Akt ($P < 0.001$) and p70S6K ($P < 0.05$) relative to control, and similarly increased ERK in control and ethanol-exposed livers relative to vehicle (Fig. 3). In contrast, myriocin failed to increase and normalize IRS-1 expression in ethanol-exposed livers.

ANOVA tests demonstrated significant intergroup differences with respect to $p^{Y1162/Y1163}$–insulin receptor ($F = 4.58$; $P = 0.013$) (Fig. 4a), p^{S473}–Akt ($F = 8.2$; $P = 0.0009$) (Fig. 4e), p^{S9}–GSK-3β ($F = 6.89$; $P = 0.0023$) (Fig. 4f), and $p^{T421/S424}$–p70S6K ($F = 7.94$; $P = 0.001$) (Fig. 4h). In contrast, ethanol or myriocin treatment had no significant effects on the expression levels of $p^{Y1135/Y1136}$–IGF-1R (Fig. 4b), p^{S312}–IRS-1 (Fig. 4c), $p^{T202/Y204}$–ERK1/2 (Fig. 4d), or p^{T246}–PRAS40 (Fig. 4g). Post hoc Tukey's multiple comparison test

revealed significantly reduced levels of p^{S473}–Akt ($P < 0.01$) and increased levels of p^{S9}–GSK-3β ($P = 0.05$) and $p^{T421/S424}$–p70S6K ($P < 0.01$) in ethanol + vehicle relative to control + vehicle livers. The reduced levels of p^{T246}–PRAS40 in ethanol-exposed livers did not reach statistical significance. Myriocin increased p^{S473}–Akt and decreased $p^{Y1162/Y1163}$–insulin receptor ($P < 0.05$) and $p^{T421/S424}$–p70S6K ($P < 0.01$) in ethanol-treated livers (relative to vehicle). Levels of the phosphorylated forms of insulin receptor, IGF-1 receptor, IRS-1, ERK1/2, Akt, PRAS40, and p70S6K were similar in myriocin-treated control and ethanol-exposed livers. In contrast, p^{S9}–GSK-3β expression was significantly higher in ethanol-exposed, myriocin-treated livers versus corresponding control livers (Fig. 4f).

ANOVA tests demonstrated significant intergroup differences with respect to the calculated relative levels of protein phosphorylation: $p^{Y1162/Y1163}$/total insulin receptor ($F = 4.96$; $P = 0.009$) (Supporting Information Fig. S1a), p^{S312}/total IRS-1 ($F = 23.82$; $P < 0.0001$) (Supporting Information Fig. S1c), p^{S473}/total Akt ($F = 12.02$; $P = 0.001$) (Supporting Information Fig. S1e), p^{S9}/total GSK-3β ($F = 3.11$; $P = 0.049$) (Supporting Information Fig. S1f), and $p^{T421/S424}$/total p70S6K ($F = 43.44$; $P < 0.0001$) (Supporting Information Fig. S1h). In contrast, ethanol or myriocin treatment had no significant effects on the relative expression of $p^{Y1135/Y1136}$/total IGF-1R (Supporting Information Fig. S1b), $p^{T202/Y204}$/total ERK1/2(Supporting Information Fig. S1d), or p^{T246}/total PRAS40 (Supporting Information Fig. S1g). Post hoc Tukey's multiple comparison test revealed that myriocin significantly reduced the calculated relative levels of $p^{Y1162/Y1163}$/total insulin receptor ($P < 0.01$), p^{S473}/total Akt ($P < 0.001$), and $p^{T421/S424}$/total p70S6K ($P < 0.001$) relative to ethanol + vehicle and/or control + vehicle. The mean relative levels of p^{S312}/total IRS-1 were significantly higher in ethanol + vehicle and ethanol + myriocin groups relative to both control groups ($P < 0.001$). Otherwise, the relative levels of protein phosphorylation were similar in myriocin-treated control and ethanol-exposed livers (Supporting Information Fig. S1).

Effects of myriocin on AAH–Notch signaling networks in chronic ALD

Duplex probe-based qRT-PCR assays revealed significant effects of ethanol and/or myriocin treatment on AAH ($F = 4.11$; $P = 0.017$) (Fig. 5a), Jagged-1 ($F = 8.25$; $P = 0.0006$), hypoxia-inducible factor 1α (HIF-1α) ($F = 5.25$; $P = 0.063$) (Fig. 5c), and HES-1 ($F = 2.99$; $P = 0.05$) (Fig. 5e). Post hoc Tukey multiple comparison tests demonstrated that chronic ethanol feeding inhibited hepatic expression of AAH ($P < 0.05$; Fig. 5a) and HES-1 ($P < 0.05$; Fig. 5e) but increased expression of Jagged-1 ($P < 0.05$) and HIF-1α ($P < 0.05$) relative to control (+ vehicle). Myriocin treatment resulted in similar (not significantly different) levels of AAH, HIF-1α, and HES-1 in control and ethanol-exposed livers, but did not increase AAH mRNA in the ethanol + vehicle group. In contrast, neither Jagged-1 (Fig. 5b) nor Notch-1 (Fig. 5d) expression was significantly modulated by myriocin.

Duplex ELISAs, in which immunoreactivity was normalized to large ribosomal protein (RPLPO), were used to measure AAH (A85G6 antibody), Humbug (A85E6 antibody), Notch-1, Jagged-1, and proliferating cell nuclear antigen (PCNA) (Fig. 6). ANOVA tests demonstrated significant effects of ethanol or myriocin on AAH ($F = 37.24$; $P < 0.0001$ (Fig. 6a), Humbug ($F = 38.14$; $P < 0.0001$) (Fig. 6b), Notch-1 ($F = 17.64$; $P < 0.0001$) (Fig. 6c), Jagged-1 ($F = 41.20$; $P < 0.0001$) (Fig. 6d), and PCNA ($F = 36.02$; $P < 0.0001$) (Fig.

6e). Tukey's multiple comparison tests demonstrated that chronic ethanol feeding significantly reduced hepatic expression of AAH ($P < 0.001$), Humbug ($P < 0.001$), Notch-1 ($P < 0.05$), Jagged-1 ($P < 0.001$), and PCNA ($P < 0.001$) relative to vehicle-treated control livers. Myriocin significantly increased the expression of all five proteins in the ethanol group and all but PCNA in the control group. The net effect was to render the expression of all five proteins similar in control livers and ethanol-exposed, myriocin-treated livers. The findings with respect to AAH were corroborated by Western blot analysis (Fig. S2).

Discussion

Study rationale and objectives

Progressive liver degeneration is mediated by compromised hepatocellular growth, survival, glucose utilization, energy metabolism, and protein synthesis,[9,13] which are needed for regeneration, repair, and remodeling after injury. Although peroxisome proliferator-activated receptor (PPAR) agonists, which are insulin sensitizers that have anti-inflammatory actions, can prevent or reverse histopathologic, ultrastructural, biochemical, and molecular abnormalities in chronic ALD,[4,47,48] not all aspects of ALD are resolved. In particular, ceramide load and ER stress remain elevated,[40] setting the stage for ALD to progress due to persistent insulin/IGF resistance and inhibition of target genes and signaling molecules that regulate liver remodeling. Therefore, additional therapeutic approaches are needed. Herein, we evaluated responses to a ceramide inhibitor in an established model of ALD.

Ceramide inhibitor effects on ALD pathology

Myriocin treatment, which significantly reduced hepatic ceramide levels, substantially reduced the severity of steatohepatitis, despite continued ethanol exposure. Myriocin resolved the hepatic steatosis, architectural disarray, sinusoidal dilatation, and, to a large extent, the inflammation. Persistence of inflammatory and necrotic/apoptotic foci (although small and scattered) corresponds with ongoing injury caused by daily ethanol exposures. Overall, the findings suggest that ceramide accumulation in liver is a critical mediator of ALD. This conclusion is consistent with the known cytotoxic effects of ceramides, including activation of proinflammatory cytokines, as well as the inhibition of insulin signaling through Akt, which regulates hepatocellular metabolism, survival, and growth.[37,38] Therefore, by reducing hepatic ceramide, liver structure and function in ALD can be restored. Furthermore, as many drugs require liver metabolism for detoxification, ceramide inhibitor therapy could raise the threshold of drug toxicity in ALD.

Effects of myriocin on ethanol-impaired signaling through insulin receptor, IRS-1, Akt, and ERK

Previous studies demonstrated that chronic ALD is associated with hepatic insulin and IGF resistance.[9,13,40] The spectrum of abnor malities includes alterations in trophic factor, receptor, and/or insulin receptor substrate (IRS) protein and/or gene expression, as well as reduced activation of ERK, MAPK, and PI3K-Akt. Ethanol-impaired signaling through ERK is associated with reduced regenerative capacity of the liver,[8] whereas reduced Akt leads to impaired cell survival, remodeling, motility, and metabolism.[4,8,12] Herein we again

demonstrate that chronic ethanol feeding broadly impairs hepatic insulin signaling mechanisms, from receptor to IRS-1, and beyond, including molecules downstream of Akt, specifically PRAS40 and P70S6K.[10,47] Myriocin reduced or abolished most ethanol-associated impairments in insulin signaling, suggesting that in chronic ALD, impairments in insulin signaling are mediated in part by hepatic ceramide accumulation. These findings highlight the importance of targeting dysregulated lipid metabolism and lipotoxicity in the clinical management of ALD.

Myriocin reverses ethanol–mediated inhibition of AAH expression

Previous studies demonstrated that AAH, and its highly homologous truncated *N*-terminus homologue, Humbug,[18,19] are stimulated by insulin and IGF[14,26,28,29] and inhibited by ethanol.[3,29–31] Although ethanol inhibits AAH's mRNA, it more prominently decreases AAH's protein expression due to activation of GSK-3β. GSK-3β phosphorylates AAH and renders it susceptible to proteolytic degradation.[27,30] PPAR agonist enhancement of insulin signaling in experimental ALD restores AAH protein expression and hepatic architecture.[4,15,47] Herein, we show similar positive efffects of myriocin on AAH protein in ALD. However, since GSK-3β activation was not significantly modulated by myriocin, the mechanism of enhanced AAH protein expression most likely differed from the effects of PPAR agonists. One potential mechanism is that the myriocin effect on AAH may have been mediated by reduced hepatocellular stress along with pro-apoptotic, inflammatory, and proteolytic functions[49] owing to increased signaling through Akt.

Myriocin reverses ethanol-mediated inhibition of Notch signaling mechanisms

Notch signaling is activated by a ligand, such as Delta or Serrate (Jagged), binding to Notch receptors on the cell surface.[23] Subsequent proteolytic cleavage of Notch releases its intracellular domain, which trans-locates to the nucleus, where it binds to transcriptional regulators such as CSL, displacing corepressors and recruiting coactivators.[23,24] The net effect is to increase expression of target genes, including those coding for HES and HES-related proteins.[50] Notch signaling is regulated by AAH,[14,26,27] and both Notch and Jagged have the consensus sequence for AAH hydroxylation.[21,22] AAH's catalytic activity promotes Notch's translocation to the nucleus, cell adhesion, and cell motility,[17,29] yet AAH expression and function are stimulated by insulin/IGF[15,28] and inhibited by ethanol.[30] In addition, previous studies showed that AAH and Notch cross-talk with HIF-1α and that HIF-1α expression is regulated by insulin/IGF and stimulated by oxidative stress and ethanol.[26]

Herein, we show that myriocin had no significant effects on the mRNA levels of AAH, Notch-1, Jagged-1, or HIF-1α and instead increased expression of AAH, Humbug, Notch-1, and Jagged-1 proteins in both control and ethanol-exposed livers. Corresponding with the anticipated increases in Notch signaling, HES-1 mRNA levels were increased by myriocin treatment of ethanol-exposed livers. HES-1 is a downstream target of Notch signaling, and the finding of normalized/increased HES-1 expression in ethanol + myriocin-treated livers reflects increased Notch activation by myriocin. The increased expression of HIF-1α in ethanol-exposed livers is consistent with previous observations.[26] In essence, ethanol-

impaired AAH–Notch signaling mechanisms and growth potential of the liver (PCNA expression) were restored by myriocin treatment.

Conclusions

The findings suggest that aberrant ceramide accumulation plays a major role in the pathogenesis of ALD. Moreover, although insulin sensitizer drugs, such as PPAR agonists[4,47,48] and anti-inflammatory agents,[10] can prevent or reverse many aspects of ALD, their failure to completely resolve the disease process could be due to persistently high levels of hepatic ceramides.[47] The results suggest that monotherapy with ceramide inhibitors can restore hepatic architecture and function in chronic ALD because they normalize hepatic ceramide levels and thereby reduce lipotoxicity, inflammation, and impairments in insulin/IGF-1 signaling and gene expression. Moreover, ceramide inhibitors support signaling through pathways that activate AAH–Notch networks utilized for structural remodeling of the liver after injury.

Supplementary Material

Refer to Web version on PubMed Central for supplementary material.

Acknowledgments

Supported by AA-11431, AA-12908, and 5T32DK060415 from the National Institutes of Health.

References

1. McCullough AJ, O'Shea RS, Dasarathy S. Diagnosis and management of alcoholic liver disease. J. Dig. Dis. 2011; 12:257–62. [PubMed: 21091932]
2. O'Shea RS, Dasarathy S, McCullough AJ. Alcoholic liver disease. Hepatology. 2010; 51:307–28. [PubMed: 20034030]
3. de la Monte SM, Yeon JE, Tong M, et al. Insulin resistance in experimental alcohol-induced liver disease. J. Gastroenterol. Hepatol. 2008; 23:e477–86. [PubMed: 18505416]
4. Pang M, de la Monte SM, Longato L, et al. PPARδ agonist attenuates alcohol-induced hepatic insulin resistance and improves liver injury and repair. J. Hepatol. 2009; 50:1192–201. [PubMed: 19398227]
5. Longato L, Ripp K, Setshedi M, et al. Insulin resistance, ceramide accumulation, and endoplasmic reticulum stress in human chronic alcohol-related liver disease. Oxid. Med. Cell Longev. 2012; 2012:479348. [PubMed: 22577490]
6. Kaplowitz N, Ji C. Unfolding new mechanisms of alcoholic liver disease in the endoplasmic reticulum. J. Gastroenterol. Hepatol. 2006; 21(Suppl. 3):S7–9. [PubMed: 16958678]
7. Lieber CS. Alcoholic fatty liver: its pathogenesis and mechanism of progression to inflammation and fibrosis. Alcohol. 2004; 34:9–19. [PubMed: 15670660]
8. He J, de la Monte S, Wands JR. Acute ethanol exposure inhibits insulin signaling in the liver. Hepatology. 2007; 46:1791–800. [PubMed: 18027876]
9. Ronis MJ, Wands JR, Badger TM, de la Monte SM, Lang CH, Calissendorff J. Alcohol-induced disruption of endocrine signaling. Alcohol. Clin. Exp. Res. 2007; 31:1269–85. [PubMed: 17559547]
10. Setshedi M, Longato L, Petersen DR, et al. Limited therapeutic effect of N-acetylcysteine on hepatic insulin resistance in an experimental model of alcohol-induced steatohepatitis. Alcohol. Clin. Exp. Res. 2011; 35:2139–51. [PubMed: 21790669]

11. Roberts RA, James NH, Cosulich SC. The role of protein kinase B and mitogen-activated protein kinase in epidermal growth factor and tumor necrosis factor alpha-mediated rat hepatocyte survival and apoptosis. Hepatology. 2000; 31:420–7. [PubMed: 10655266]
12. Derdak Z, Lang CH, Villegas KA, et al. Activation of p53 enhances apoptosis and insulin resistance in a rat model of alcoholic liver disease. J. Hepatol. 2011; 54:164–72. [PubMed: 20961644]
13. de la Monte, SM. Alcohol-induced liver and brain degeneration: roles of insulin resistance, toxic ceramides, and endoplasmic reticulum stress.. In: Watson, RR.; Preedy, VR.; Zipadi, S., editors. Alcohol, Nutrition, and Health Consequences. Humana Press; New York: 2012. p. 507-22.
14. Cantarini MC, de la Monte SM, Pang M, et al. Aspartyl-asparagyl beta hydroxylase over-expression in human hepatoma is linked to activation of insulin-like growth factor and Notch signaling mechanisms. Hepatology. 2006; 44:446–57. [PubMed: 16871543]
15. de la Monte SM, Tamaki S, Cantarini MC, et al. Aspartyl-(asparaginyl)-beta-hydroxylase regulates hepatocellular carcinoma invasiveness. J. Hepatol. 2006; 44:971–83. [PubMed: 16564107]
16. Ince N, de la Monte SM, Wands JR. Overexpression of human aspartyl (asparaginyl) beta-hydroxylase is associated with malignant transformation. Cancer Res. 2000; 60:1261–6. [PubMed: 10728685]
17. Lavaissiere L, Jia S, Nishiyama M, et al. Overexpression of human aspartyl(asparaginyl)beta-hydroxylase in hepatocellular carcinoma and cholangiocarcinoma. J. Clin. Invest. 1996; 98:1313–23. [PubMed: 8823296]
18. Jia S, McGinnis K, VanDusen WJ, et al. A fully active catalytic domain of bovine aspartyl (asparaginyl) beta-hydroxylase expressed in Escherichia coli: characterization and evidence for the identification of an active-site region in vertebrate alpha-ketoglutarate-dependent dioxygenases. Proc. Natl Acad. Sci. U.S.A. 1994; 91:7227–31. [PubMed: 8041771]
19. Jia S, VanDusen WJ, Diehl RE, et al. cDNA cloning and expression of bovine aspartyl (asparaginyl) beta-hydroxylase. J. Biol. Chem. 1992; 267:14322–7. [PubMed: 1378441]
20. Feriotto G, Finotti A, Breveglieri G, Treves S, Zorzato F, Gambari R. Transcriptional activity and Sp 1/3 transcription factor binding to the P1 promoter sequences of the human AβH-J-J locus. FEBS J. 2007; 274:4476–90. [PubMed: 17681019]
21. Dinchuk JE, Focht RJ, Kelley JA, et al. Absence of post-translational aspartyl beta-hydroxylation of epidermal growth factor domains in mice leads to developmental defects and an increased incidence of intestinal neoplasia. J. Biol. Chem. 2002; 277:12970–7. [PubMed: 11773073]
22. Dahlback B, Hildebrand B, Linse S. Novel type of very high affinity calcium-binding sites in beta-hydroxyasparagine-containing epidermal growth factor-like domains in vitamin K-dependent protein S. J. Biol. Chem. 1990; 265:18481–9. [PubMed: 2145284]
23. Bray S, Bernard F. Notch targets and their regulation. Curr. Top. Dev. Biol. 2010; 92:253–75. [PubMed: 20816398]
24. D'Souza B, Meloty-Kapella L, Weinmaster G. Canonical and non-canonical Notch ligands. Curr. Top. Dev. Biol. 2010; 92:73–129. [PubMed: 20816393]
25. Hirata H, Yoshiura S, Ohtsuka T, et al. Oscillatory expression of the bHLH factor Hes1 regulated by a negative feedback loop. Science. 2002; 298:840–3. [PubMed: 12399594]
26. Lawton M, Tong M, Gundogan F, Wands JR, de la Monte SM. Aspartyl-(asparaginyl) beta-hydroxylase, hypoxia-inducible factor-alpha and Notch cross-talk in regulating neuronal motility. Oxid. Med. Cell Longev. 2010; 3:347–56. [PubMed: 21150341]
27. Silbermann E, Moskal P, Bowling N, Tong M, de la Monte SM. Role of aspartyl-(asparaginyl)-beta-hydroxylase mediated notch signaling in cerebellar development and function. Behav. Brain Funct. 2010; 6:68. [PubMed: 21050474]
28. Lahousse SA, Carter JJ, Xu XJ, Wands JR, de la Monte SM. Differential growth factor regulation of aspartyl-(asparaginyl)-beta-hydroxylase family genes in SH-Sy5y human neuroblastoma cells. BMC Cell Biol. 2006; 7:41. [PubMed: 17156427]
29. Carter JJ, Tong M, Silbermann E, et al. Ethanol impaired neuronal migration is associated with reduced aspartyl-asparaginyl-beta-hydroxylase expression. Acta Neuropathol. (Berl). 2008; 116:303–15. [PubMed: 18478238]

30. de la Monte SM, Tong M, Carlson RI, et al. Ethanol inhibition of aspartyl-asparaginyl-beta-hydroxylase in fetal alcohol spectrum disorder: potential link to the impairments in central nervous system neuronal migration. Alcohol. 2009; 43:225–40. [PubMed: 19393862]
31. Gundogan F, Elwood G, Longato L, et al. Impaired placentation in fetal alcohol syndrome. Placenta. 2008; 29:148–57. [PubMed: 18054075]
32. Cohen JI, Nagy LE. Pathogenesis of alcoholic liver disease: interactions between parenchymal and non-parenchymal cells. J. Dig. Dis. 2011; 12:3–9. [PubMed: 21091930]
33. de la Monte SM, Longato L, Tong M, DeNucci S, Wands JR. The liver–brain axis of alcohol-mediated neurodegeneration: role of toxic lipids. Int. J. Environ. Res. Public Health. 2009; 6:2055–75. [PubMed: 19742171]
34. Kao Y, Youson JH, Holmes JA, Al-Mahrouki A, Sheridan MA. Effects of insulin on lipid metabolism of larvae and metamorphosing landlocked sea lamprey, Petromyzon marinus. Gen. Comp. Endocrinol. 1999; 114:405–14. [PubMed: 10336828]
35. Ding WX, Manley S, Ni HM. The emerging role of autophagy in alcoholic liver disease. Exp. Biol. Med. (Maywood). 2011; 236:546–56. [PubMed: 21478210]
36. Holland WL, Summers SA. Sphingolipids, insulin resistance, and metabolic disease: new insights from in vivo manipulation of sphingolipid metabolism. Endocr. Rev. 2008; 29:381–402. [PubMed: 18451260]
37. Bourbon NA, Sandirasegarane L, Kester M. Ceramide-induced inhibition of Akt is mediated through protein kinase Czeta: implications for growth arrest. J. Biol. Chem. 2002; 277:3286–92. [PubMed: 11723139]
38. Hajduch E, Balendran A, Batty IH, et al. Ceramide impairs the insulin-dependent membrane recruitment of protein kinase B leading to a loss in downstream signalling in L6 skeletal muscle cells. Diabetologia. 2001; 44:173–83. [PubMed: 11270673]
39. Nogueira TC, Anhe GF, Carvalho CR, Curi R, Bordin S, Carpinelli AR. Involvement of phosphatidylinositol-3 kinase/AKT/PKCζ/λ pathway in the effect of palmitate on glucose-induced insulin secretion. Pancreas. 2008; 37:309–15. [PubMed: 18815554]
40. Ramirez T, Longato L, Dostalek M, Tong M, Wands JR, de la Monte SM. Insulin resistance, ceramide accumulation and endoplasmic reticulum stress in experimental chronic alcohol-induced steatohepatitis. Alcohol Alcohol. 2013; 48:39–52. [PubMed: 22997409]
41. Garcia-Ruiz C, Colell A, Mari M, et al. Defective TNF-alpha-mediated hepatocellular apoptosis and liver damage in acidic sphingomyelinase knockout mice. J. Clin. Invest. 2003; 111:197–208. [PubMed: 12531875]
42. Liangpunsakul S, Sozio MS, Shin E, et al. Inhibitory effect of ethanol on AMPK phosphorylation is mediated in part through elevated ceramide levels. Am. J. Physiol. Gastrointest. Liver Physiol. 2010; 298:G1004–12. [PubMed: 20224005]
43. Anderson N, Borlak J. Molecular mechanisms and therapeutic targets in steatosis and steatohepatitis. Pharmacol. Rev. 2008; 60:311–57. [PubMed: 18922966]
44. Kuznetsov JN, Leclerc GJ, Leclerc GM, Barredo JC. AMPK and Akt determine apoptotic cell death following perturbations of one-carbon metabolism by regulating ER stress in acute lymphoblastic leukemia. Mol. Cancer Ther. 2011; 10:437–47. [PubMed: 21262957]
45. Glaros EN, Kim WS, Wu BJ, et al. Inhibition of atherosclerosis by the serine palmitoyl transferase inhibitor myriocin is associated with reduced plasma glycosphingolipid concentration. Biochem. Pharmacol. 2007; 73:1340–6. [PubMed: 17239824]
46. de la Monte SM, Re E, Longato L, Tong M. Dysfunctional pro-ceramide, ER stress, and insulin/IGF signaling networks with progression of Alzheimer's disease. J. Alzheimers Dis. 2012; 30:S217–29. [PubMed: 22297646]
47. Ramirez T, Tong M, Chen WC, Nguyen QG, Wands JR, de la Monte SM. Chronic alcohol-induced hepatic insulin resistance and endoplasmic reticulum stress ameliorated by peroxisome-proliferator activated receptor-delta agonist treatment. J. Gastroenterol. Hepatol. 2013; 28:179–87. [PubMed: 22988930]
48. de la Monte SM, Pang M, Chaudhry R, et al. Peroxisome proliferator-activated receptor agonist treatment of alcohol-induced hepatic insulin resistance. Hepatol. Res. 2011; 41:386–98. [PubMed: 21426453]

49. Summers SA. Ceramides in insulin resistance and lipotoxicity. Prog. Lipid Res. 2006; 45:42–72. [PubMed: 16445986]

50. Kageyama R, Ohtsuka T, Hatakeyama J, Ohsawa R. Roles of bHLH genes in neural stem cell differentiation. Exp. Cell Res. 2005; 306:343–8. [PubMed: 15925590]

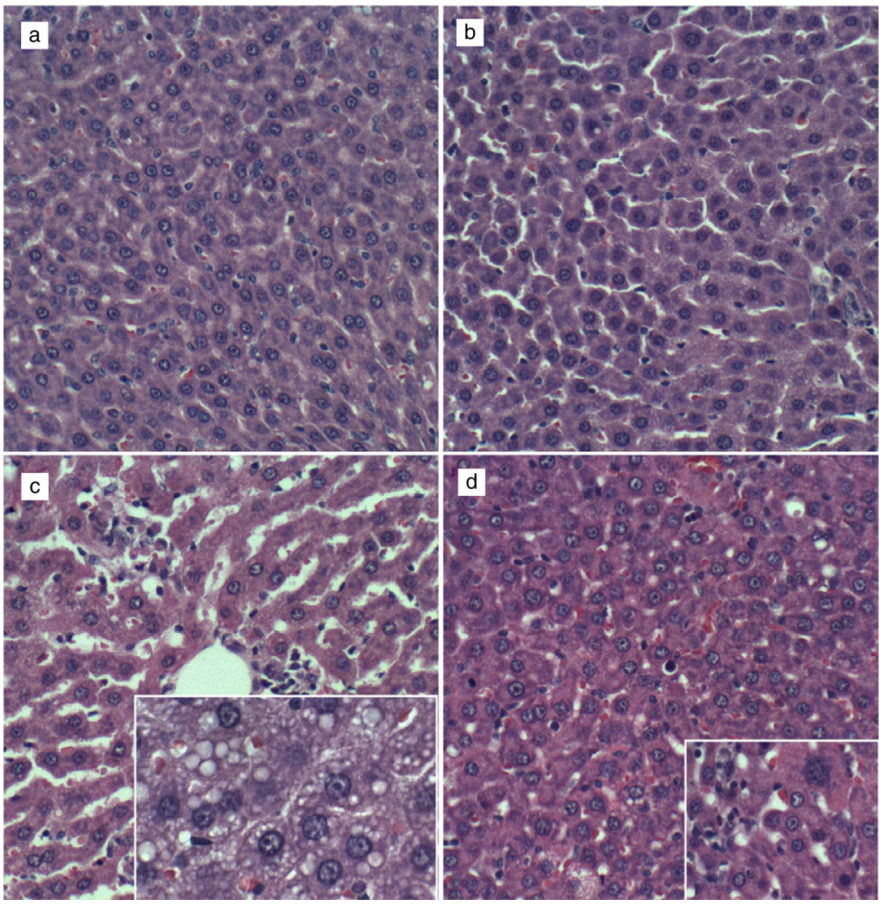

Figure 1.

Histopathologic features of experimental alcohol-induced steatohepatitis—effects of myriocin treatment. Adult male Long–Evans rats were fed with isocaloric liquid diets containing 0% (control) or 37% ethanol (caloric content) for 8 weeks and were treated with vehicle or myriocin 3 times per week over the last 5 weeks of the experiment. Paraformaldehyde-fixed paraffin-embedded 5-μm-thick sections of liver were stained with HE. (a) Control livers had regular cordlike architectures and uniform hepatocyte structure. (b) Myriocin treatment had minimal discernible effect on hepatic architecture in control rats. (c) Ethanol-exposed livers exhibited foci of lymphomononuclear cell inflammation (upper left and center), apoptotic bodies, and prominent microvesicular steatosis (clear cytoplasmic vacuoles—inset). (d) Myriocin treatment nearly normalized hepatic architecture in ethanol-fed rats, although apoptosis and mild inflammation persisted (inset).

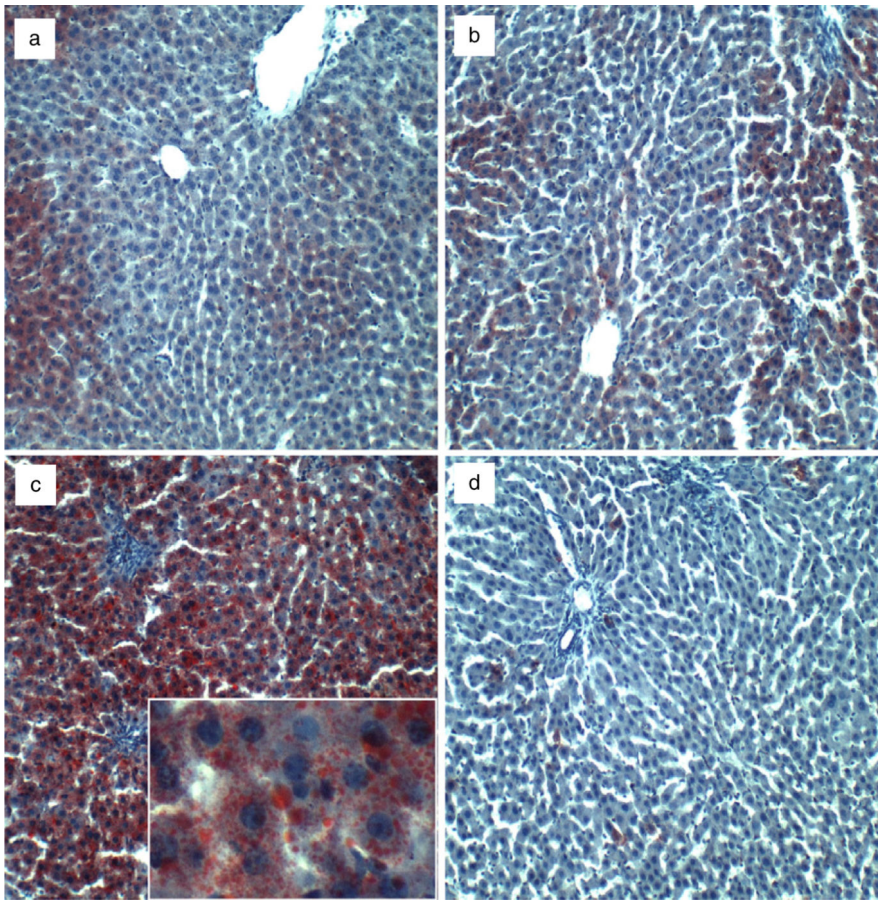

Figure 2.

Increased hepatic steatosis in experimental chronic alcohol-relaed liver disease—effects of myriocin treatment. Cryostat sections of paraformaldehydefixed livers from (a) control + vehicle, (b) control + myriocin, (c) ethanol + vehicle, and (d) ethanol + myriocin groups were stained with Oil Red O to detect cytoplasmic lipid accumulation (red punctate or vesicular labeling—inset in c).

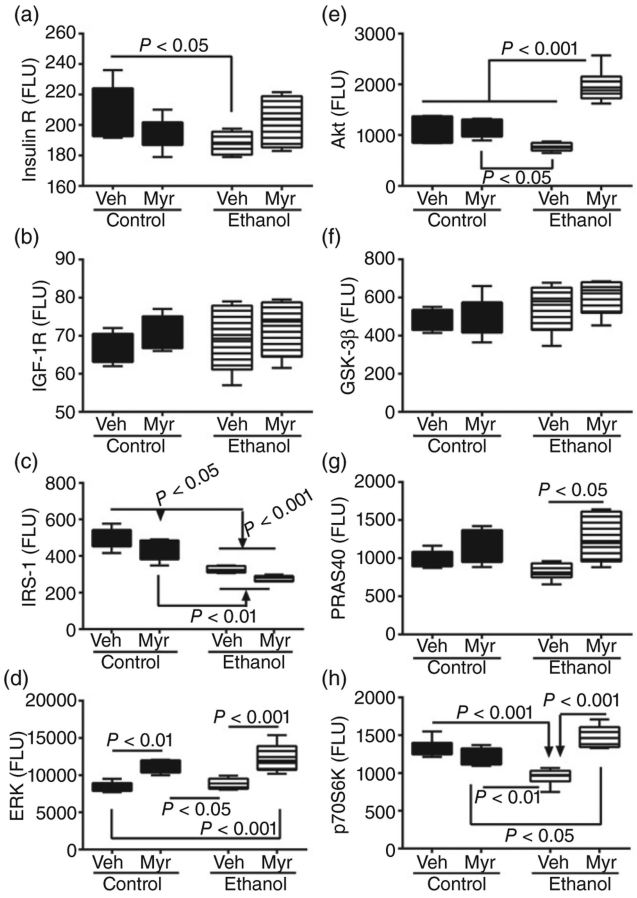

Figure 3.

Chronic ethanol feeding and myriocin treatment effects on hepatic insulin, insulin growth factor (IGF) and insulin receptor substrate (IRS) signaling mechanisms. Liver tissue from control and chronic ethanol-fed rats that were treated with vehicle (Veh) or myriocin (Myr) was used to measure (a) insulin receptor, (b) IGF-1 receptor, (c) IRS-1, (d) extracellular signal-regulated kinases 1 and 2, (e) Akt, (f) glycogen synthase kinase 3β, (g) proline-rich Akt substrate 40 kDa, and (h) p70S6 kinase by multiplex or single-plex ELISA. Results were normalized to protein content in reactions; $n = 8$ or 10 samples per group. Box plots depict medians (horizontal bars), 95% confidence intervals (upper and lower limits of boxes), and ranges (stems). Intergroup comparisons were made by repeated-measures one-way ANOVA with post hoc Tukey tests. FLU, fluorescent light units.

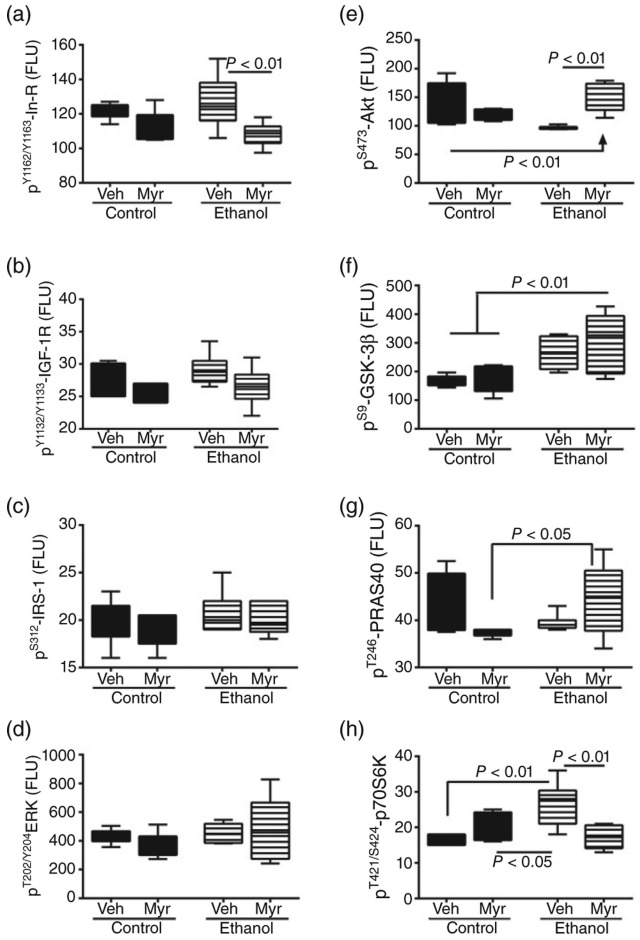

Figure 4.

Chronic ethanol feeding and myriocin treatment effects on phosphorylated insulin, IGF and IRS signaling molecules in liver. Liver tissue from control and chronic ethanol-fed rats that were treated with vehicle or myriocin was used to measure (a) $^{pYpY1162/1163}$-insulin receptor, (b) $^{pYpY1135/1136}$-IGF-1 receptor, (c) ^{pS312}-IRS-1, (d) $^{pT202/Y204}$-ERK1/2, (e) ^{pS473}-Akt, (f) ^{pS9}-GSK3b, (g) ^{pT246}-PRAS40, and (h) ^{pT246pS112}-p70S6K by multiplex or single-plex ELISA. Results normalized to protein content in the reactions. Box plots depict medians (horizontal bars), 95% confidence intervals (upper and lower limits of boxes), and ranges (stems). Inter-group comparisons were made by repeated measures one-way ANOVA with post-hoc Tukey tests of significance.

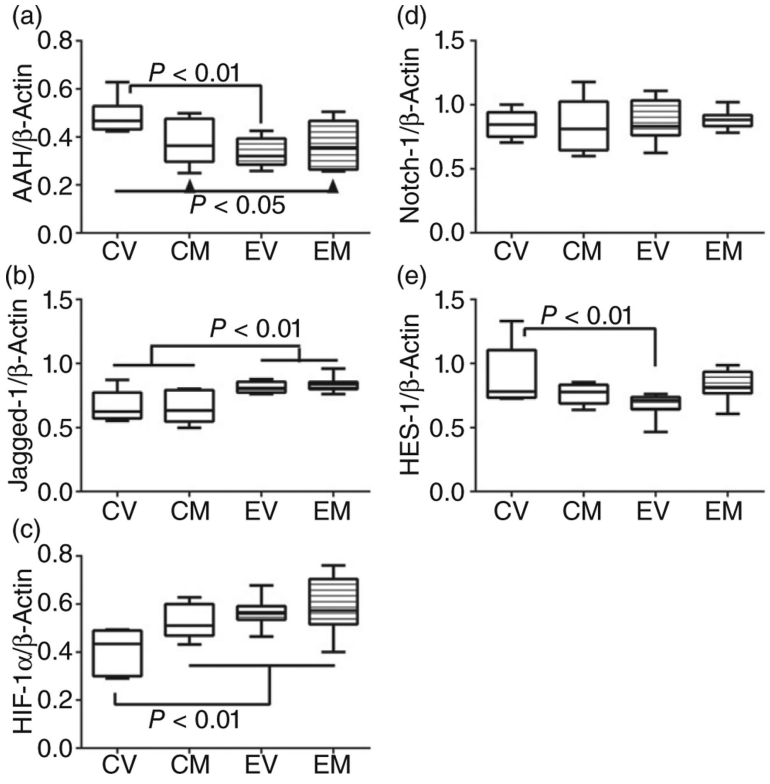

Figure 5.

Effects of chronic ethanol exposure and myriocin treatment on aspartyl-asparaginyl-β-hydroxylase (AAH) and Notch signaling-related mRNAs in liver. Livers from control and chronic ethanol-fed rats that were treated with vehicle or myriocin were used to measure (a) AAH, (b) Jagged-1, (c) hypoxia-inducible factor 1α, (d) Notch-1, and (e) Hairy–Enhancer of Split-1 mRNA levels in probe hydrolysis-based quantitative real-time polymerase chain reaction assays. Results were normalized to β-actin, which was measured simultaneously. Intergroup comparisons were made using the calculated mRNA/β-actin ratios. CV, control + vehicle; CM, control + myriocin; EV, ethanol + vehicle; EM, ethanol + myriocin; $n = 8$ or 10 samples per group. Box plots depict medians (horizontal bars), 95% confidence intervals (upper and lower limits of boxes), and ranges (stems). Intergroup comparisons were made by repeated-measures one-way ANOVA with post hoc Tukey tests of significance.

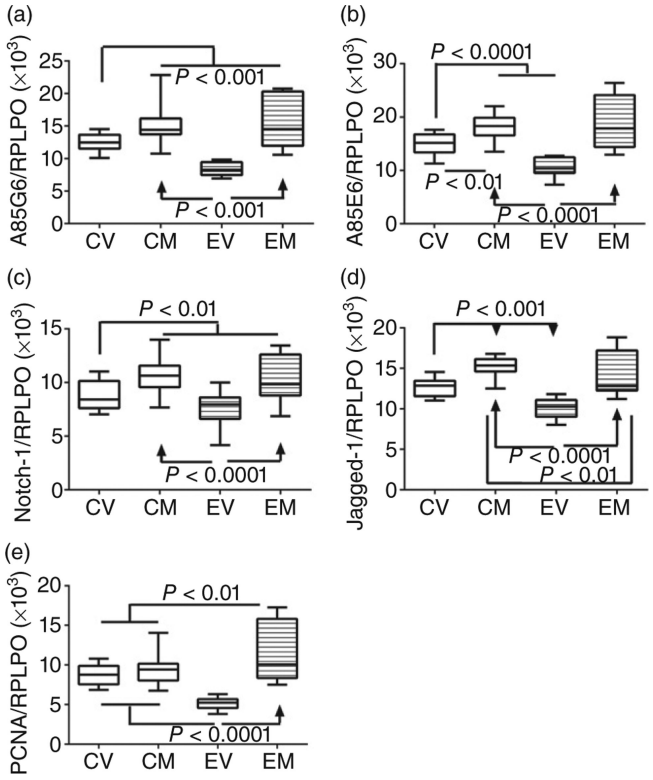

Figure 6.

Effects of chronic ethanol exposure and myriocin treatment on aspartyl-asparaginyl-β-hydroxylase (AAH) and Notch signaling molecules in liver. Livers from control and chronic ethanol-fed rats that were treated with vehicle or myriocin were used to measure (a) AAH-A85G6, (b) AAH/Humbug-A85E6, (c) Notch-1, (d) Jagged-1, and (e) proliferating cell nuclear antigen immunoreactivity by duplex ELISAs. Results were normalized to large ribosomal protein (RPLPO), which was measured in the same wells. Intergroup comparisons were made using calculated protein/RPLPO ratios. CV, control + vehicle; CM, control + myriocin; EV, ethanol + vehicle; EM, ethanol + myriocin; n = 8 or 10 samples per group. Box plots depict medians (horizontal bars), 95% confidence intervals (upper and lower limits of boxes), and ranges (stems). Intergroup comparisons were made by repeated-measures one-way ANOVA with post hoc Tukey tests of significance.